

See discussions, stats, and author profiles for this publication at: <https://www.researchgate.net/publication/282731632>

Automatic Artery–Vein Separation from Thoracic CT Images Using Integer Programming

Conference Paper · October 2015

DOI: 10.1007/978-3-319-24571-3_5

CITATION

1

READS

196

6 authors, including:



Michael Pienn

Ludwig Boltzmann Institute for Lung Vascula...

19 PUBLICATIONS 71 CITATIONS

SEE PROFILE



Zoltán Bálint

Babeş-Bolyai University

61 PUBLICATIONS 564 CITATIONS

SEE PROFILE



Andrea Olschewski

Ludwig Boltzmann Institute for Lung Vascula...

170 PUBLICATIONS 2,127 CITATIONS

SEE PROFILE



Martin Urschler

Ludwig Boltzmann Institute for Clinical-Fore...

87 PUBLICATIONS 555 CITATIONS

SEE PROFILE

Some of the authors of this publication are also working on these related projects:



Automatic age estimation from skeletal and dental MRI data using machine learning [View project](#)



The influence of erythropoietin on growth and survival in non-small cell lung cancer cell lines [View project](#)

All content following this page was uploaded by [Martin Urschler](#) on 11 October 2015.

The user has requested enhancement of the downloaded file. All in-text references [underlined in blue](#) are added to the original document and are linked to publications on ResearchGate, letting you access and read them immediately.

Automatic Artery-Vein Separation from Thoracic CT Images using Integer Programming

Christian Payer^{1,2,*}, Michael Pienn², Zoltán Bálint²,
Andrea Olschewski², Horst Olschewski³, and Martin Urschler^{4,1}

¹ Institute for Computer Graphics and Vision,

BioTechMed, Graz University of Technology, Austria

² Ludwig Boltzmann Institute for Lung Vascular Research, Graz, Austria

³ Department of Pulmonology, Medical University of Graz, Austria

⁴ Ludwig Boltzmann Institute for Clinical Forensic Imaging, Graz, Austria

Abstract. Automated computer-aided analysis of lung vessels has shown to yield promising results for non-invasive diagnosis of lung diseases. In order to detect vascular changes affecting arteries and veins differently, an algorithm capable of identifying these two compartments is needed. We propose a fully automatic algorithm that separates arteries and veins in thoracic computed tomography (CT) images based on two integer programs. The first extracts multiple subtrees inside a graph of vessel paths. The second labels each tree as either artery or vein by maximizing both, the contact surface in their Voronoi diagram, and a measure based on closeness to accompanying bronchi. We evaluate the performance of our automatic algorithm on 10 manual segmentations of arterial and venous trees from patients with and without pulmonary vascular disease, achieving an average voxel based overlap of 94.1% (range: 85.0% – 98.7%), outperforming a recent state-of-the-art interactive method.

1 Introduction

The automatic extraction of vascular tree structures is highly relevant in medical image analysis. Especially the investigation of the pulmonary vascular tree, the complex lung vessel network responsible for oxygen uptake and carbon dioxide release, is of great interest in clinical practice. Applications include detection of early stage pulmonary nodules [1], pulmonary embolism [2], or pulmonary hypertension [3]. The recent trend towards quantitative pulmonary computer-aided diagnosis (CAD) was enabled by the rapid progress in medical imaging technologies, with state-of-the-art computed tomography (CT) scanners allowing depiction of anatomical structures in the lung at a sub-millimeter level at low radiation doses. This remarkable resolution can help in CAD of diseases like chronic obstructive pulmonary disease [4] or pulmonary hypertension [5]. However, the higher amount of data leads to an increased demand for fully automatic

* We thank Peter Kullnig for radiological support, Vasile Fóris for medical support and data analysis and Martin Wurm for his help in the manual artery-vein separations.

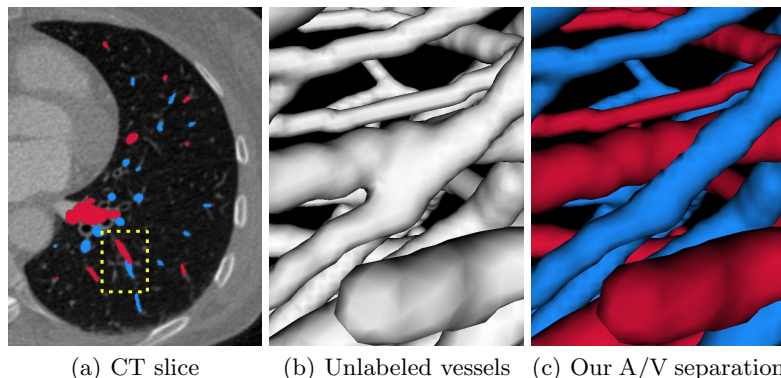


Fig. 1. Thoracic CT case where arteries (blue) and veins (red) are close to each other.

extraction and computer-aided quantitative analysis of pulmonary structures, including the automated separation of arterial and venous trees (see Fig. 1). This can improve the diagnosis of lung diseases affecting both trees differently.

Automatic artery-vein (A/V) separation is a very complex problem, due to the similar intensity values of both vessel trees in CT. Further, the pulmonary arterial and venous trees are intertwined and the vessels are in close proximity, making their distinction even harder. Most of the few existing A/V separation algorithms start with vessel segmentation, often using tubularity filters combined with region growing or fast marching methods based on seed points [6]. The work of [7] proposes to solely detect pulmonary arteries by using the anatomical constraint that arteries usually run along the bronchi, whereas the method of [8] involves global structural information by constructing a minimum-spanning-tree from weights derived from local vessel geometry measures and a cutting step for A/V separation. However, using this method, an interactive refinement is often necessary to finalize the separation. In [9] A/V separation utilizes the close proximity of arteries and veins. By morphological operations with differently sized kernels, equal intensity structures are split and locally separated regions are traced. [10] extended this method with a GUI enabling efficient refinement. Another promising method is [11], who formulate an automatic voxel labeling problem based on root detection for both trees. However, it requires a training step and, due to locally restricted image features, it still has problems near the hilum of the lung, i.e. where arteries and veins are in close proximity.

In this work we present a novel, automatic A/V separation algorithm for thoracic CT images, which requires no manual correction and takes the global structural information about vascular trees as well as local features like vessel orientation and bronchus proximity into account. Based on a vessel segmentation step we formulate both the extraction of subtrees and the labeling of arteries and veins as integer programs. We evaluate our method on a database of 10 thoracic CT images with manually segmented A/V trees as a reference and demonstrate the benefits of our method compared to the state-of-the-art method in [8].

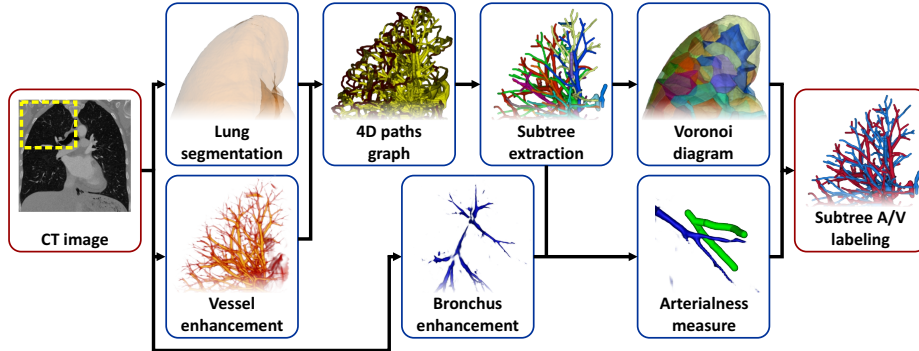


Fig. 2. Overview of our proposed A/V separation algorithm.

2 Method

Our proposed algorithm for A/V separation from contrast-enhanced thoracic CT images is shown in Fig. 2. After a lung segmentation from [5], subsequent processing is performed for both lungs independently. A multi-scale vessel enhancement filter [12] produces a vessel orientation estimate as well as a 4D tubularity image for the three spatial coordinates and the radius. Next, we calculate a graph $G = (V, E)$ of regularly spaced local maxima V of the vessel enhanced image, which are connected by edges E in a local neighborhood similar to [13]. For every edge, a path between its two endpoints is extracted, which minimizes the geodesic distance, penalizing small tubularity values along the path [12]. To drastically prune these edges, a filtering step is performed removing all paths that fully contain any other path. The resulting graph still contains many spurious edges, but also the real arterial and venous vessel paths. These are subsequently organized in subtrees and separated using two integer programs.

2.1 Subtree Extraction

In order to identify anatomically meaningful vascular trees and prepare the input for A/V separation, we contribute a novel method to extract a set of connected subtrees from the overcomplete maxima graph G , using an optimization procedure based on an integer program. Different from [13], we do not need explicitly declared root nodes, but include their search into the optimization. Formally, we find multiple tree-like structures in G , defined by edge tuples $\langle e_{ij}, t_{ij} \rangle$, where binary variable $t_{ij} = 1$ indicates that the path from node i to node j is active, i.e. contained in one of the resulting subtrees. The quadratic objective function is a sum of weights $w_{ijk} \in \mathbb{R}$ of adjacent oriented edge pairs described by t_{ij} and t_{jk} to model the tree structure, and a term controlling the creation of subtrees formalized by a binary variable $r_{ij} \in \{0, 1\}$ indicating if e_{ij} is a root of a subtree:

$$\begin{aligned}
& \arg \min_{t,r} \sum_{e_{ij}, e_{jk} \in E} w_{ijk} t_{ij} t_{jk} + \sigma \sum_{e_{ij} \in E} r_{ij} \\
\text{s.t.} \quad & \sum_{e_{hi} \in E} t_{hi} + r_{ij} \geq t_{ij}, \quad \sum_{e_{hi} \in E} t_{hi} + r_{ij} \leq 1, \quad \forall e_{ij} \in E \\
& t_{ij} \geq r_{ij}, \quad t_{ij} + t_{ji} \leq 1,
\end{aligned} \tag{1}$$

The linear constraints in (1) enforce tree-like structures by ensuring that an active edge $t_{ij} = 1$ has exactly one predecessor $t_{hi} = 1$ in the set e_{hi} of all preceding edges, or is a root node $r_{ij} = 1$. The fourth constraint guarantees that a directed edge and its opposite are not active simultaneously. With $\sigma \in \mathbb{R}_0^+$ the number of created subtrees is globally controlled, where in contrast to [13] we allow growing of numerous subtrees throughout the whole local maxima graph, and select the best root nodes of anatomically meaningful subtrees implicitly. The key component of the integer program is the weight w_{ijk} of adjacent oriented edge pairs. It consists of three parts, the first one derived from the costs of traveling along the path from node i to k via j according to the tubularity measure, the second one penalizing paths with strong orientation changes computed by the mean of the dot products of directions along a path, and the final part penalizing radius increases from start node i to end node k . While all other components are positive, a global parameter $\delta \in \mathbb{R}^-$ is further added to w_{ijk} to allow for negative weights, otherwise the trivial solution, i.e. no extracted paths and subtrees, would always minimize the objective function (1).

After minimizing the objective function, the integer program results in a list of individual connected subtrees, which is post-processed to locate the anatomical branching points instead of local tubularity maxima.

2.2 Subtree A/V Labeling

Next, each individual subtree is labeled as either artery or vein using two anatomical properties. First, we exploit that arteries and veins are roughly uniformly distributed in the lung. The second property uses the fact, that bronchi run parallel and in close proximity to arteries, as previously proposed in [7]. The main contribution of our work lies in a novel optimization model calculating the final A/V labeling by an integer program, that assigns to every individual subtree t_i either $a_i = 1$ (artery) or $v_i = 1$ (vein). This is achieved by maximizing

$$\begin{aligned}
& \arg \max_{a,v} \sum_{t_i, t_j \in T} a_i v_j w_{ij}^{border} + \lambda \sum_{t_i \in T} a_i w_i^{artery} \\
\text{s.t.} \quad & a_i + v_i = 1, \quad \forall t_i \in T,
\end{aligned} \tag{2}$$

where the first term counts the number of voxels $w_{ij}^{border} \in \mathbb{R}_0^+$ on the contact surface between artery and vein regions modeled by a generalized Voronoi diagram. For each voxel inside the lung segmentation this Voronoi diagram determines the nearest subtree. By maximizing the sum of all w_{ij}^{border} of neighboring artery

and vein regions, a uniform distribution of arteries and veins throughout the whole lung is ensured. The second term of (2) uses a measure of arterialness $w_i^{artery} \in \mathbb{R}_0^+$ for every tree t_i to incorporate a distinction between arteries and veins. Our arterialness measure is inspired by [7], but instead of searching for bronchus points in the input CT image, we employ the multi-scale tubularity filter from [12] for locating dark on bright bronchus structures. At each voxel along the segments of a subtree, we locally search for similarly oriented bronchial structures giving high tubularity response in a plane orthogonal to the vessel direction. After fitting a line through all bronchus candidate locations of a vessel segment, we compute an arterialness measure from their distance and deviation in direction. This gives higher values for arteries running closer and in parallel to bronchi, while veins, typically more distant and deviating stronger from the bronchus direction, will receive lower values. The arterialness value w_i^{artery} of a tree t_i is the sum of all arterialness values of its vessel segments. Finally, the constraint from (2) ensures, that not both labels are active at the same time for the same tree t_i . A factor λ weights the sums. The result of solving this integer program is the final labeling of arteries and veins for all subtrees.

3 Experimental Setup and Results

Experimental Setup: To validate our algorithm, we used 10 datasets from patients (6 female/4 male) with and without lung vascular disease who underwent thoracic contrast-enhanced, dual-energy CT examinations. The CT scans were acquired either with a Siemens Somatom Definition Flash (D30f reconstruction kernel) or with a Siemens Somatom Force (Qr40d reconstruction kernel) CT scanner. The size of the isotropic 0.6mm CT volumes was $512 \times 512 \times 463$ pixels.

Manual reference segmentations of all 10 patients, that include pulmonary artery and left atrium, as well as A/V trees down to a vessel diameter of 2mm, were created requiring 5–8 h per dataset. These data served as basis for validating our algorithm together with a re-implementation of [8], which is similar to our proposed method, as it extracts and labels subtrees. The interactive step of [8], i.e. the final A/V labeling of subtrees, was done manually by looking for connections to the heart for every subtree. Similarly, we additionally performed user-defined labeling of the extracted subtrees of our algorithm, to evaluate the A/V labeling part. As the compared segmentations may differ substantially in the included vessel voxels, we compared only those voxels which are present in the segmentation and the manual reference.

The development and testing platform for our C++ algorithm consisted of a Windows 7 Intel Core i5-4670 @ 3.40 GHz with 16 GB RAM. For multi-scale vessel enhancement and 4D path extraction, the publicly available code from [12] was used. Gurobi Optimizer¹ was applied to solve integer programs. The parameters $\sigma = 0.2$ and $\delta = -0.2$ were determined empirically within a few try-outs providing satisfactory results for the subtree extraction. The parameter $\lambda = 6.0$ was determined by grid search, as the A/V labeling is not time consuming.

¹ Gurobi Optimizer Version 6.0 with academic license from <http://www.gurobi.com/>

Table 1. Overlap ratio in % of automatic, Park et al. [8] and user-defined (UD) labeling methods with manual reference segmentations for the 10 datasets.

Patient #	1	2	3	4	5	6	7	8	9	10	μ
Automatic	95.0	93.3	98.4	87.3	97.4	85.0	95.0	98.7	98.5	92.4	94.1
Park et al. [8]	90.2	93.9	91.2	90.4	91.9	88.0	90.6	94.7	95.3	93.3	91.9
UD labeling	99.1	99.4	98.6	98.5	97.9	97.6	99.2	99.8	98.6	99.1	98.8

Results: The automatic algorithm generated an average of 1210 individual vessel segments, composed of 619 arteries and 591 veins, with diameters ranging from 2 to 10mm. The average voxel-based overlap of correct labels for all 10 datasets between automatic and manual reference segmentation was 94.1%. The re-implementation of [8] achieved 91.9%, whereas the user-defined subtree labeling based on the output of our subtree extraction achieved an overlap of 98.8%. The individual values are listed in Table 1, with two datasets visualized in Fig. 3.

Furthermore, in order to evaluate the subtree A/V labeling in more detail, we validated our automatic segmentation against the user-defined labeling (Table 2). The average ratio of voxels, where arteries and veins were switched (misabeled) was 4.9%. As additional voxels cannot be added by the manual labeling, the number of mistakenly detected vessels can be quantified as well. The average ratio of misclassified structures (non-vessel), i.e., the ratio of voxels that are not in the manually labeled result, but present in the automatic one, was 1.7%.

The average time needed for generating a single, fully automatic A/V segmentation with our unoptimized method was 5 hours, while [8] required 0.5 hours of computation time with additional 2 hours of interaction time.

Table 2. Comparison of user-defined subtree labeling and fully automatic segmentation for the 10 datasets. The amount of mislabeled vessel voxels (Mislabeled) and the amount of detected structures, which are not vessels (Non-vessel) is provided in %.

Patient #	1	2	3	4	5	6	7	8	9	10	μ
Mislabeled	3.9	6.1	0.2	11.6	1.8	10.4	4.6	1.4	0.6	7.9	4.9
Non-vessel	5.1	0.2	1.4	2.2	4.7	3.0	0.1	0.3	0.4	0.0	1.7

4 Discussion and Conclusion

Our proposed novel algorithm for separating arteries and veins in thoracic CT images achieves a higher average correct overlap compared to the method of [8], although the latter method includes explicit manual correction, while our approach is fully automated. We assume that our integer program is better modeling the anatomical constraints involved in A/V separation compared to the

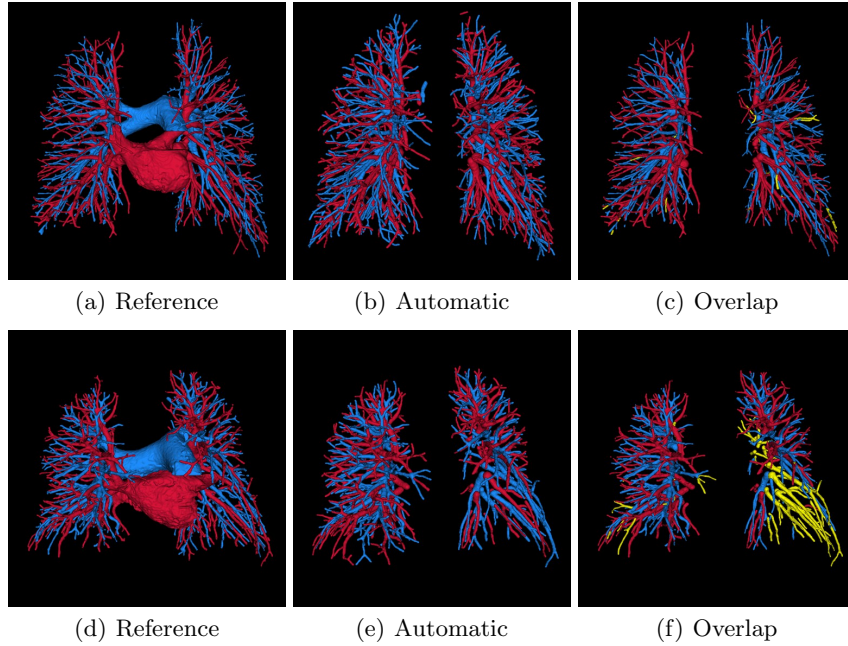


Fig. 3. Visualization of reference segmentation (left), automatic segmentations (center) and their overlap (right). Only voxels, that are set in both segmentations, are visualized in the overlap image. Red: vein, blue: arteries, yellow: disagreement between segmentations. Top row: 98.4% agreement (#3), bottom row: 85% agreement (#6).

minimum-spanning-tree of [8] by exploiting the uniform distribution of arteries and veins throughout the lungs as well as proximity and similar orientation of arteries and bronchi. Our extracted vascular subtrees are very well separated, which can be observed in Fig. 3 or by comparing the user-defined labeling with the manual reference in Table 2. Furthermore, our main contribution, the automatic A/V labeling step, removes the need for manual post-processing.

We observed that mislabeled subtrees often are neighbors in the generalized Voronoi diagram, due to the maximization of their contact surfaces. This may lead to switched labels of all subtrees within a lung lobe. Therefore, restricting the uniform distribution of arteries and veins to lung lobes instead of whole lungs could further improve performance and robustness. Because of the lack of a standardized dataset and openly available A/V separation algorithms, our algorithm was only compared to the most recently published work in [8]. The evaluation of our algorithm on a larger dataset is ongoing. As our algorithm is not optimized in its current state, we expect that improvements in runtime are still possible. Another interesting idea could be to combine subtree extraction and labeling into one integer program, like in [14]. We conclude, that our novel method provides an opportunity to become an integral part of computer aided diagnosis of lung diseases.

References

1. [Murphy, K., van Ginneken, B., Schilham, A.M.R., de Hoop, B.J., Gietema, H.A., Prokop, M.: A large-scale evaluation of automatic pulmonary nodule detection in chest CT using local image features and k-nearest-neighbour classification. *Med. Image Anal.* **13**\(5\) \(2009\) 757–770](#)
2. [Masutani, Y., MacMahon, H., Doi, K.: Computerized detection of pulmonary embolism in spiral CT angiography based on volumetric image analysis. *IEEE Trans. Med. Imaging* **21**\(12\) \(2002\) 1517–1523](#)
3. [Linguraru, M.G., Pura, J.A., Van Uitert, R.L., Mukherjee, N., Summers, R.M., Minniti, C., Gladwin, M.T., Kato, G., Machado, R.F., Wood, B.J.: Segmentation and quantification of pulmonary artery for noninvasive CT assessment of sickle cell secondary pulmonary hypertension. *Med. Phys.* **37**\(4\) \(2010\) 1522–1532](#)
4. [Estépar, R.S.J., Kinney, G.L., Black-Shinn, J.L., Bowler, R.P., Kindlmann, G.L., Ross, J.C., Kikinis, R., Han, M.K., Come, C.E., Diaz, A.A., Cho, M.H., Hersh, C.P., Schroeder, J.D., Reilly, J.J., Lynch, D.A., Crapo, J.D., Wells, J.M., Dransfield, M.T., Hokanson, J.E., Washko, G.R.: Computed tomographic measures of pulmonary vascular morphology in smokers and their clinical implications. *Am. J. Respir. Crit. Care Med.* **188**\(2\) \(2013\) 231–239](#)
5. [Helmberger, M., Pienn, M., Urschler, M., Kullnig, P., Stollberger, R., Kovacs, G., Olschewski, A., Olschewski, H., Bálint, Z.: Quantification of tortuosity and fractal dimension of the lung vessels in pulmonary hypertension patients. *PLoS One* **9**\(1\) \(2014\) e87515](#)
6. [van Rikxoort, E.M., van Ginneken, B.: Automated segmentation of pulmonary structures in thoracic computed tomography scans: a review. *Phys. Med. Biol.* **58** \(2013\) R187–R220](#)
7. [Bülow, T., Wiemker, R., Blaffert, T., Lorenz, C., Renisch, S.: Automatic extraction of the pulmonary artery tree from multi-slice CT data. In: *Proc. SPIE 5746, Med. Imaging Physiol. Funct. Struct. from Med. Images.* \(2005\) 730–740](#)
8. [Park, S., Lee, S.M., Kim, N., Seo, J.B., Shin, H.: Automatic reconstruction of the arterial and venous trees on volumetric chest CT. *Med. Phys.* **40**\(7\) \(2013\) 071906](#)
9. [Saha, P.K., Gao, Z., Alford, S.K., Sonka, M., Hoffman, E.A.: Topomorphologic separation of fused isointensity objects via multiscale opening: Separating arteries and veins in 3-D pulmonary CT. *IEEE Trans. Med. Imaging* **29**\(3\) \(2010\) 840–851](#)
10. [Gao, Z., Grout, R.W., Holtze, C., Hoffman, E.A., Saha, P.K.: A new paradigm of interactive artery/vein separation in noncontrast pulmonary CT imaging using multiscale topomorphologic opening. *IEEE Trans. Biomed. Eng.* **59**\(11\) \(2012\) 3016–3027](#)
11. [Kitamura, Y., Li, Y., Ito, W., Ishikawa, H.: Adaptive higher-order submodular potentials for pulmonary artery-vein segmentation. In: *Proc. Fifth Int. Work. Pulm. Image Anal.* \(2013\) 53–61](#)
12. [Benmansour, F., Türetken, E., Fua, P.: Tubular Geodesics using Oriented Flux: An ITK Implementation. *The Insight Journal* \(2013\)](#)
13. [Türetken, E., Benmansour, F., Andres, B., Pfister, H., Fua, P.: Reconstructing Loopy Curvilinear Structures Using Integer Programming. In: *IEEE Conf. Comput. Vis. Pattern Recognit.* \(2013\) 1822–1829](#)
14. [Robben, D., Türetken, E., Sunaert, S., Thijs, V., Wilms, G., Fua, P., Maes, F., Suetens, P.: Simultaneous Segmentation and Anatomical Labeling of the Cerebral Vasculature. *MICCAI* \(2014\) 307–314](#)